AJNR

Magnetic susceptibility artifacts in gradient-recalled echo MR imaging.

L F Czervionke, D L Daniels, F W Wehrli, L P Mark, L E Hendrix, J A Strandt, A L Williams and V M Haughton

AJNR Am J Neuroradiol 1988, 9 (6) 1149-1155
http://www.ajnr.org/content/9/6/1149

Magnetic Susceptibility Artifacts in Gradient-Recalled Echo MR Imaging

Leo F. Czervionke[1]
David L. Daniels[1]
Felix W. Wehrli[2]
Leighton P. Mark[1]
Lloyd E. Hendrix[1]
Julie A. Strandt[1]
Alan L. Williams[1]
Victor M. Haughton[1]

Artifacts related to magnetic susceptibility differences between bone and soft tissue are prevalent on gradient-recalled echo images, particularly when long echo delay times are used. These susceptibility artifacts spatially distort and artifactually enlarge bone contours. This can alter the apparent shape of the spinal canal and exaggerate the degree of spinal stenosis seen in patients with cervical spondylosis.

The effects of magnetic susceptibility artifacts in gradient echo imaging were studied in a phantom model and the results were correlated with MR images obtained in patients with cervical spondylosis.

Magnetic susceptibility is the ratio of the intensity of magnetization produced in a substance to the intensity of the applied magnetic field [1]. In other words, magnetic susceptibility is a measure of the extent a substance can be magnetized when placed in an external magnetic field. In spin echo imaging, ferromagnetic materials have high magnetic susceptibility, which alters the homogeneity of the field and results in geometric distortion of the image [2]. To a lesser extent such geometric distortion has been observed near air/tissue interfaces when gradient-recalled echoes (GRE) are used [3]. Spatial variations in magnetic or diamagnetic susceptibility cause intrinsic magnetic field gradients across the imaging voxel. Spins subjected to these gradients lose phase coherence with a concomitant attenuation in signal intensity, leading to the well-known artifactual loss of signal intensity near air-containing sinus cavities. The susceptibility differences between bone and soft tissue are less than those between air and soft tissue. However, unless the appropriate imaging parameters are selected, the susceptibility differences are sufficient to severely compromise diagnosis in GRE images of the spine. The effects of magnetic susceptibility artifacts in gradient echo imaging were studied in a phantom model and the results were correlated with MR images obtained in patients with cervical spondylosis.

Materials and Methods

A test tube phantom was designed to study the effects of magnetic susceptibility artifacts in spin echo and gradient echo pulse sequences. Two test tubes 13 mm in diameter were filled with saline and immersed in a container of saline and gelatin. Two fragments of bone were placed alongside one of the test tubes and held in position by a rubber band. A second test tube was placed in the container and was used as a control for comparison. The lower portion of each test tube was in contact with the gelatin bath and the upper portion of each tube was in contact with room air. Images were obtained in sagittal and axial planes through the test tubes using spin echo and gradient echo techniques with a standard head coil on a 1.5-T MR imager.* Imaging parameters used for obtaining the spin echo (SE) images were 2000/20, 80 (TR/TEs), 128 × 256 or 256 × 256 matrix, 1 excitation, 24-cm field of view, and 5-mm slice thickness. Parameters used for the GRE images were 200/10, 20, 30, 40 (TR/TEs), 4 excitations, 128 × 256 or 256 × 256 matrix, 24-cm field of view, and 5-mm slice thickness.

Received October 26, 1987; accepted after revision April 5, 1988.

[1] Department of Radiology, Medical College of Wisconsin. Froedtert Memorial Lutheran Hospital, 9200 W. Wisconsin Ave., Milwaukee, WI 53226. Address reprint requests to L. F. Czervionke.

AJNR 9:1149–1155, November/December 1988
0195–6108/88/0906–1149

* GE Medical Systems, Milwaukee, WI.

Three normal volunteers and five patients with the diagnosis of cervical spondylosis were studied with two different gradient echo pulse sequences: a single slice technique (GRASS*) and a multislice technique (PSI*). Parameters used to obtain the GRASS images were 200/10, 20, 30 (TR/TEs), 256 × 256 matrix, and 24-cm field of view. Parameters used for the PSI images were 750/9, 18, 27, and 36 (TR/TEs), 256 × 256 matrix, and 24-cm field of view. Patients were studied in axial and sagittal planes.

Three patients with known ferromagnetic metallic objects in the soft tissues of the neck were also studied to compare the magnetic susceptibility effects of SE and GRE techniques.

Results

T2-weighted SE and GRE images of the phantom are shown in Figure 1. In the SE sequence (Fig. 1A), the margins of the test tube were spatially mismapped (misregistered) where the test tube was in contact with air in that the portion of the test tube surrounded by air appeared shifted along the frequency-encoding axis. There was negligible spatial distortion of the test tube adjacent to the bone fragments or adjacent to the saline-gelatin bath commensurate with the smaller susceptibility difference for the latter two materials. In the GRE pulse sequence (Fig. 1B), the margins of the test tube adjacent to air were similarly distorted, particularly at the interface of air and the gelatin bath. However, the GRE images exhibited an additional effect, that of signal loss at the location of the susceptibility-induced gradients. This effect is seen near the gelatin-air boundary as well as at the margins of the bone fragments.

On axial images obtained through the phantom with SE techniques, we observed negligible distortion of the test tube margin adjacent to the bone fragments (Fig. 2). When axial GRE techniques were used, there was greater spatial distortion and signal loss adjacent to the bone fragments and test tube margins with increasing echo delay times caused by variations in magnetic susceptibility (Fig. 3). Magnetic susceptibility artifacts, while minimal, were seen with echo delay times as short as 10 msec in sagittal sections (Fig. 4).

The GRE images obtained from normal volunteers demonstrated the effect of magnetic susceptibility artifacts in the cervical spine (Fig. 5). These artifacts were seen as thin dark indistinct ridges apparently indenting the dural sac. They were most apparent on paramedian sagittal images near the vertebral laminae. These ridging artifacts were accentuated with increasing echo delay time (Fig. 5).

The effect of magnetic susceptibility artifacts in GRE images in patients with cervical spondylosis is illustrated in Figures 6 and 7. Distortion and exaggeration in the size of osteophytes were apparent when longer echo times were used. In addition, this artifactual exaggeration of the osteophytes caused the spinal canal to appear smaller than it really was. This effect on the spinal canal was most apparent on paramedial sagittal images (Fig. 7). Axial GRE images with

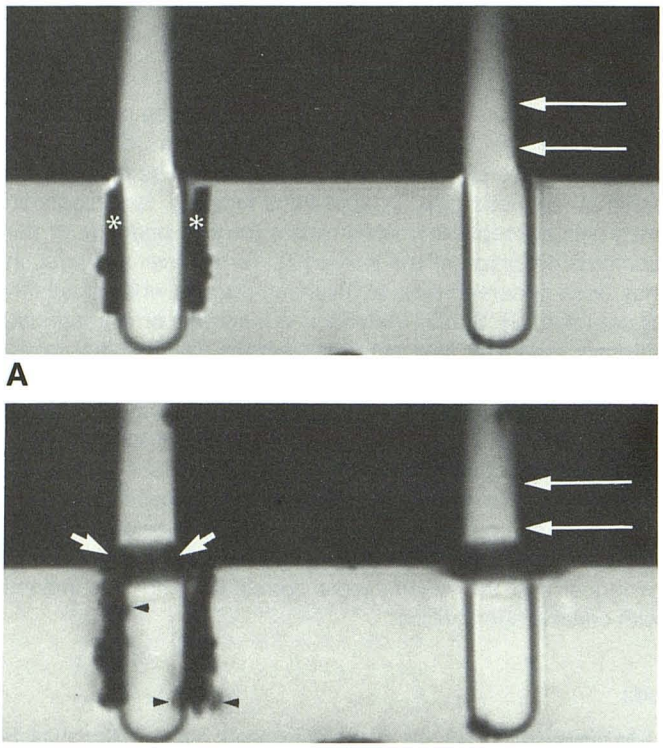

Fig. 1.—Sagittal MR images obtained through test tube phantom.
***A*, T2-weighted SE image (2000/80) shows virtually no distortion of test tube margin adjacent to bone fragments (*asterisks*).**
***B*, T2-weighted gradient-recalled echo image (200/30) using a 10° flip angle. Severe distortion and false enlargement of bone fragments (*arrowheads*) and margins of test tube are due to magnetic susceptibility artifact. Severe distortion of image also occurs where test tube contacts air and saline solution (*short arrows*). Test tubes on right without adjacent bone fragments serve as a control. Note apparent displacement of test tube (*long arrows* in *A* and *B*) along frequency-encoding axis where test tube contacts the air, representing susceptibility-induced misregistration (frequency-encoding axis is right to left in *A* and *B*).**

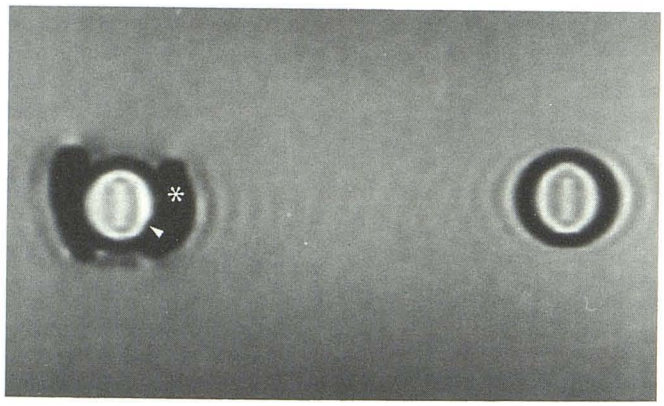

Fig. 2.—MR image obtained transversely through test tube phantom. SE image (2000/80) using 128 × 256 matrix. There is minimal distortion of test tube margin (*arrowhead*) by magnetic susceptibility artifact due to adjacent bone fragments (*asterisk*). Note also ringing artifacts adjacent to test tube margins due to data truncation. Phase-encoding axis is left to right in image.

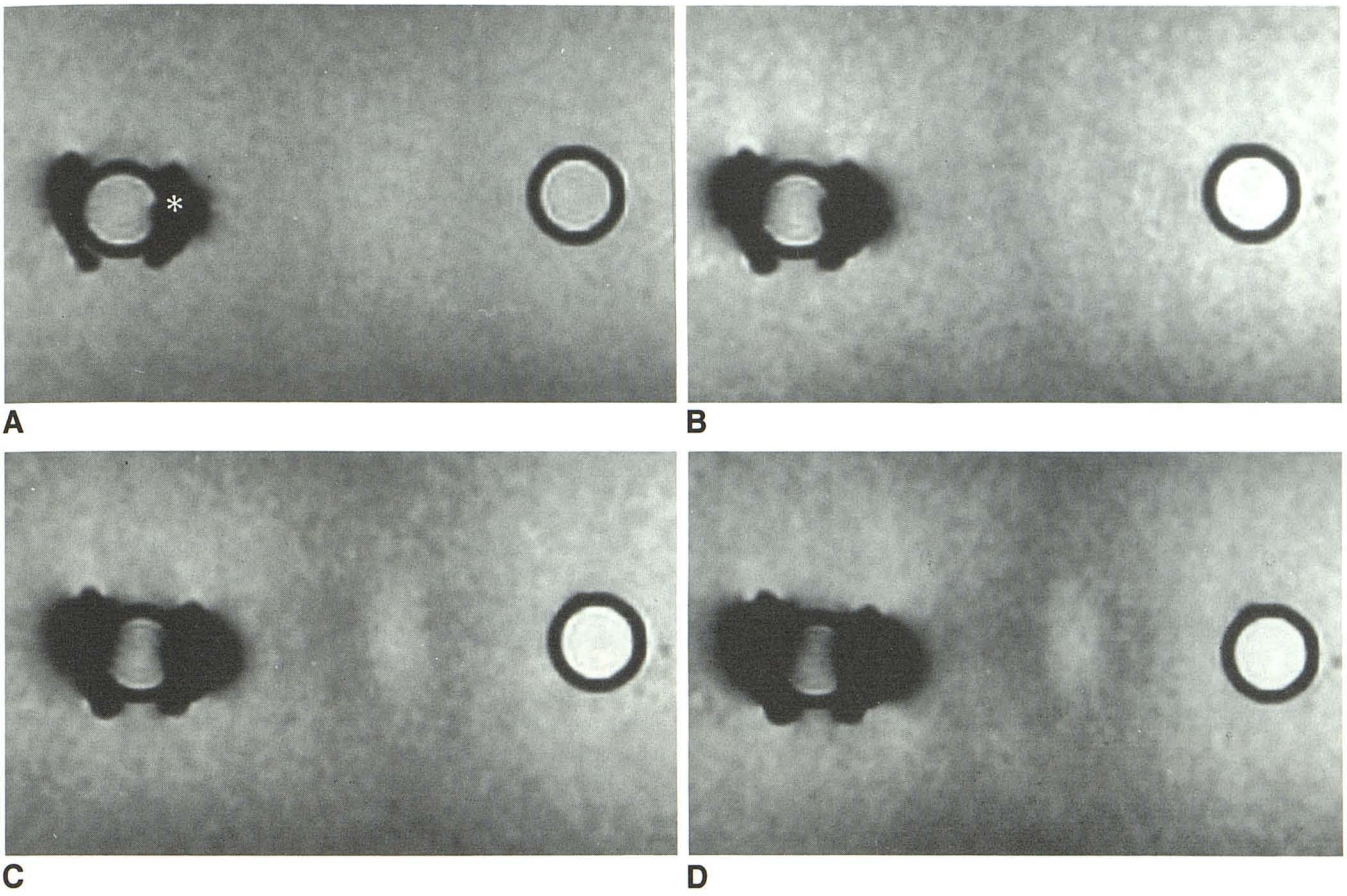

Fig. 3.—Effect of varying echo delay time in axial gradient-recalled echo imaging.
***A–D*, All images are obtained with same parameters—TR = 200, 256 × 256 matrix, 10° flip angle—except that echo times in *A–D* are 10, 20, 30, and 40, respectively. Note progressive increase in size of bone fragment artifacts (*asterisk* in *A*) and distortion of test tube margins with increasing echo delay time. Test tube on right, without any nearby bone fragments, is used for comparison.**

increasing echo delay times demonstrated false, artifactual narrowing of the neural foramina (Fig. 8). The magnetic susceptibility artifacts produced narrowing of the foramina and accentuated facet and uncinate hypertrophy. Distortion of ferromagnetic material in patients was significantly greater on GRE images compared with SE images (Fig. 9).

Discussion

Magnetic susceptibility artifacts are apparent on MR where adjacent tissues differ greatly in magnetic susceptibility, because spatial variations in magnetic susceptibility produce intrinsic magnetic field gradients in such a region of tissue (Fig. 10). For example, ferromagnetic materials are substances with very high magnetic susceptibility that distort MR images in two ways [2, 3]. First, they cause spatial mismapping (misregistration) of the object position, determined by the frequency-position relationship established by the readout gradient. This misregistration in object position occurs along the frequency-encoding axis similar to chemical shift misregistration and is observed in SE and GRE images (Fig. 1). Second, a loss of signal intensity occurs in a region where a significant difference in magnetic susceptibility exists (Fig. 9), because intrinsic gradients are produced that result in spin dephasing, which is irreversible in GRE imaging.

Since the phase build-up is proportional to the dephasing time (echo delay) [4], the signal attenuation is more apparent on T2- than T1-weighted images. However, spin dephasing adjacent to a ferromagnetic object is so pronounced that signal loss may be seen on T1-weighted images as well (Fig. 9).

A large magnetic susceptibility difference also occurs between a paramagnetic material (which strengthens the existing magnetic field) and surrounding body tissues. For example, magnetic susceptibility effects may be seen adjacent to an intracerebral hematoma [5, 6]. Most body tissues are diamagnetic (substances that weaken the magnetic field) and are magnetically fairly homogeneous (comparable magnetic

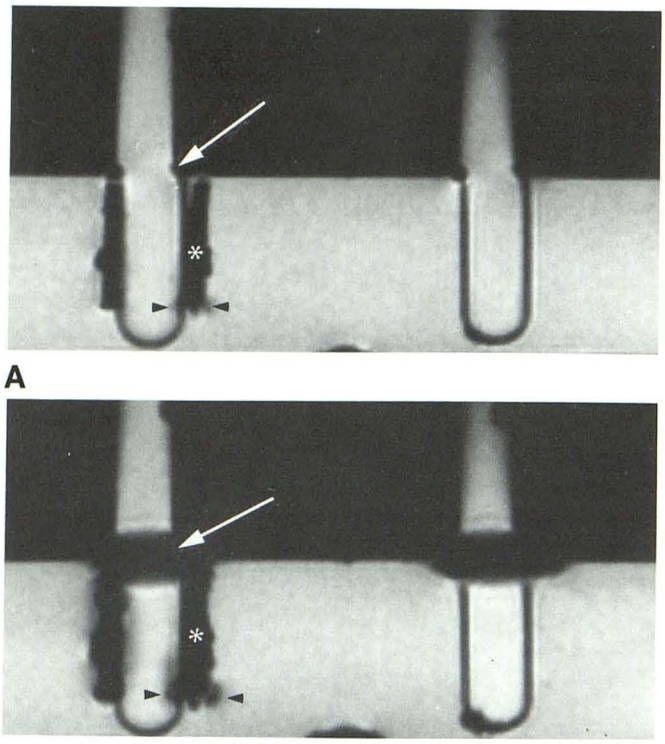

Fig. 4.—Sagittal gradient-recalled echo images of test tube phantom obtained with TR = 200, 256 × 256 matrix, and 10° flip angle. TE = 10 in *A* and TE = 40 in *B*.

A, Note minimal distortion (*arrowheads*) of shape of thickness of bone fragments (*asterisk*). There is minimal distortion of test tube adjacent to air/saline interface (*arrow*).

B, There is significantly more distortion of test tube margin (*arrow*) and bone fragments (*asterisk*).

susceptibility). Therefore, to observe magnetic susceptibility artifacts in body tissues, there must exist a significant difference in susceptibility between adjacent tissues.

A large susceptibility difference occurs between body tissues and air [3], air having very low susceptibility owing to its low density. A smaller but significant susceptibility difference exists between bone and soft tissues, such as between the skull and brain [7]. Bone is a complex substance composed of inorganic salts of calcium and phosphorus and an organic matrix. Absolute measurements of bone magnetic susceptibility have not been reported, to our knowledge [8]. However, compact cortical bone is more dense than soft tissue and this may contribute to the magnetic susceptibility effects observed near bone in the phantom (Figs. 1, 3, 4) and in the volunteers or patients (Figs. 5–8).

Magnetic susceptibility-induced misregistration along the frequency-encoding axis occurs in both SE and GRE imaging (Fig. 1) but susceptibility effects resulting in signal intensity loss are negligible in SE imaging. Inhomogeneities in the externally applied magnetic field and intrinsic tissue magnetic field gradients produced by local magnetic susceptibility variations both produce rapid spin dephasing, resulting in signal loss [3, 9, 10]. This type of spin dephasing is corrected (refocused) by the 180° pulse contained in the SE sequence, and therefore magnetic susceptibility-induced signal loss is negligible on SE images.

GRE sequences successfully refocus dephasing spins when the magnetic field is uniform across the tissue being examined. However, if the magnetic field is inhomogeneous or a significant variation in magnetic susceptibility exists, a phase dispersion will result that cannot fully be refocused by gradient reversal techniques [3], since currently available GRE sequences lack a 180° pulse.

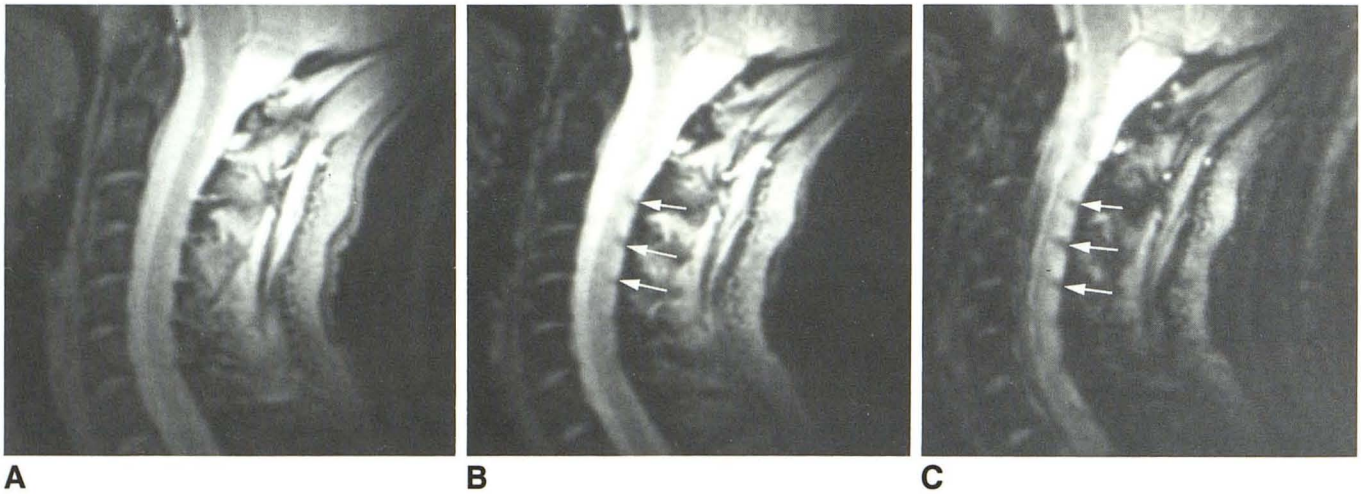

Fig. 5.—Paramedian sagittal T2-weighted gradient-recalled echo images obtained in normal volunteer with TR = 750, 256 × 256 matrix, 30° flip angle, and all other parameters identical, including slice location. *A–C* were all obtained in same acquisition series.

A, With TE = 8, no significant magnetic susceptibility artifact related to bone is seen.

B, With TE = 18, dark ridges (*arrows*) are seen to indent posterior portion of subarachnoid space.

C, With TE = 30, posterior dark ridges are more pronounced (*arrows*). In addition, motion artifact seen as prominent streaks of variable signal intensity propagated throughout the entire image are accentuated.

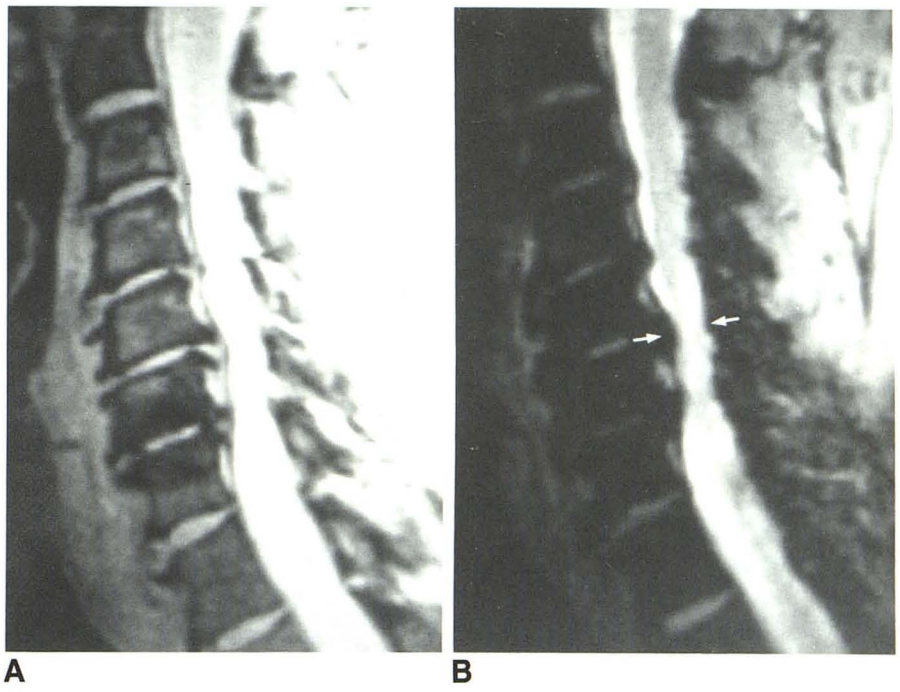

Fig. 6.—*A* and *B*, Sagittal gradient-recalled echo images of cervical spine obtained in patient with spondylosis, with TR = 750, 256 × 256 matrix, 30° flip angle in conjunction with peripheral pulse gating. TE = 9 in *A* and TE = 18 in *B*. Osteophytes projecting from anterior and posterior margins of vertebral bodies in *A* are apparently markedly distorted and enlarged in *B*. Note accentuated narrowing (*arrows* in *B*) of the spinal canal where bone ridges are most pronounced.

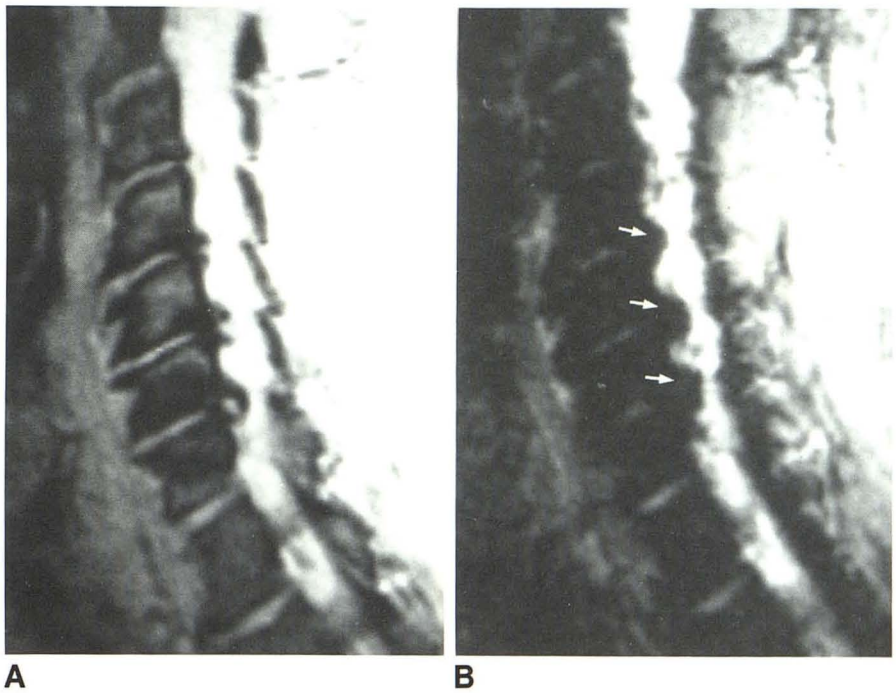

Fig. 7.—*A* and *B*, Paramedian sagittal gradient-recalled echo images of cervical spine obtained with TR = 750, 256 × 256 matrix, and 30° flip angle. TE = 9 in *A* and TE = 18 in *B*. Owing to magnetic susceptibility artifact, the apparently enlarged and distorted osteophytes (*arrows* in *B*) simulate greater narrowing of spinal canal than is actually the case.

Artifactual signal loss from magnetic susceptibility effects are greater with increasing echo delay time in GRE images (Fig. 3) because the spins have more time to dephase [3]. These artifacts are more evident on T2-weighted images, which are obtained with longer echo delay times, than on T1-weighted images.

Because of their sensitivity to dephasing phenomena in general, GRE sequences accentuate motion artifacts (motion-

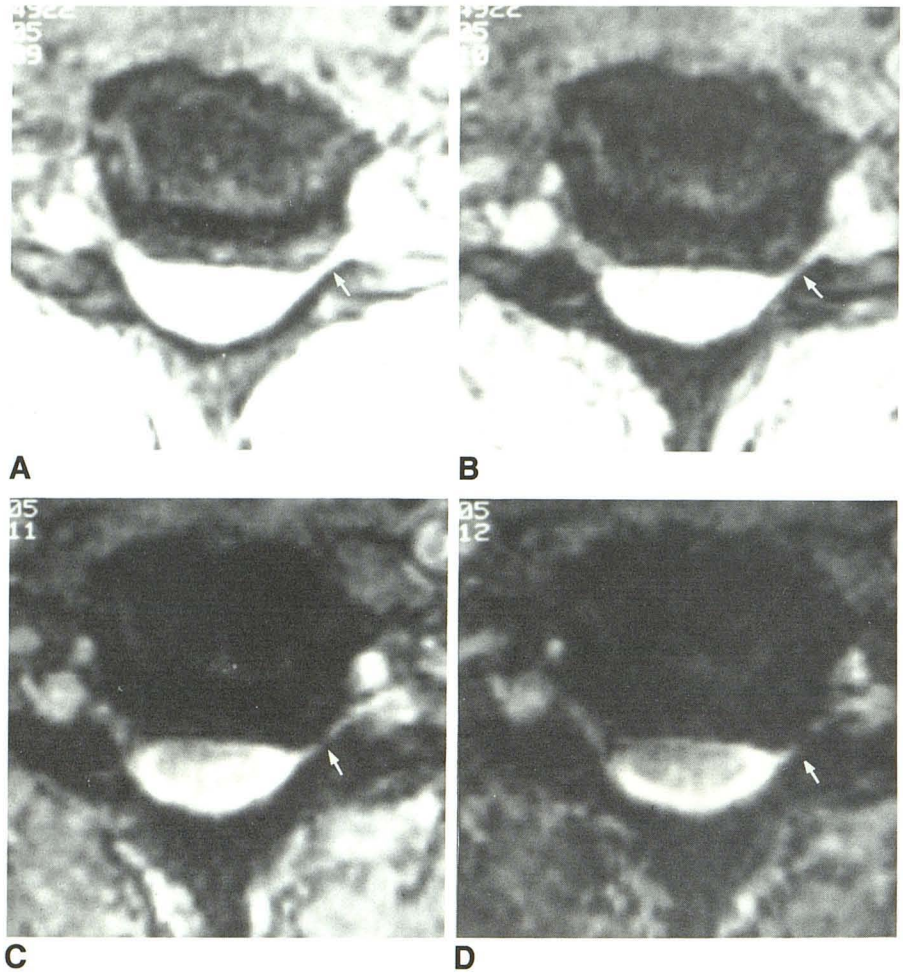

Fig. 8.—*A–D*, Axial gradient-recalled echo images obtained through cervical spine at C5–C6 level show effect of increasing echo delay time in patient with spondylosis. Parameters include TR = 750, 256 × 256 matrix, 5-mm slice thickness, and 24 cm field of view. TE = 10, 20, 30, and 40 in *A–D*, respectively. Neural foramen on patient's left (*arrow*) appears to be more narrowed with increasing echo delay time because of magnetic susceptibility artifact.

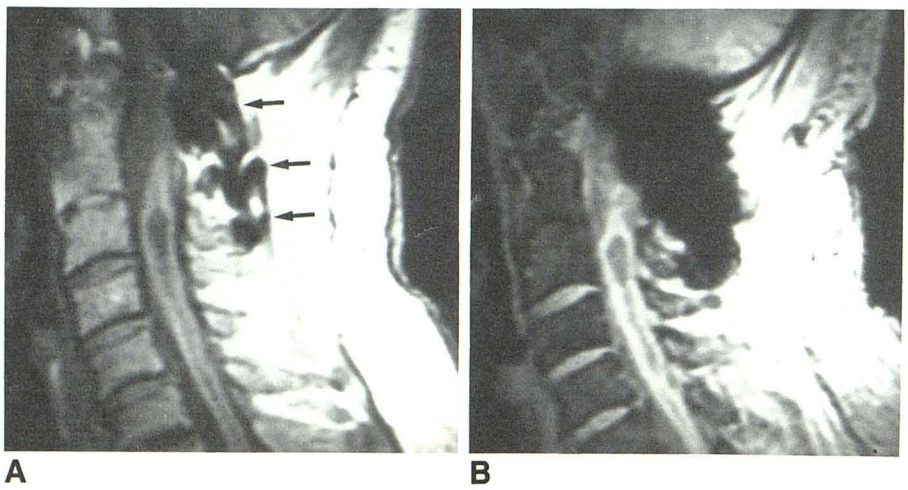

Fig. 9.—T1-weighted images of cervical spine.

***A*, T1-weighted spin echo image (800/20). Distortion of image posterior to spinal canal at C1–C2 level is due to magnetic susceptibility artifact from ferromagnetic clips (*arrows*). A syrinx cavity is evident.**

***B*, T1-weighted gradient-recalled echo image (500/10) using a 90° flip angle. Ferromagnetic metal produces even more distortion of surrounding soft tissues.**

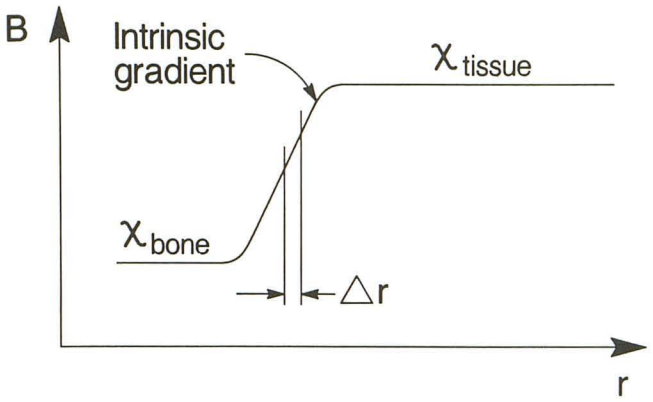

Fig. 10.—Two regions of different magnetic susceptibility (e.g., ^{x}bone and ^{x}tissue) cause an intrinsic magnetic field gradient across some imaging voxels. The result is rapid dephasing of spins and concomitant signal loss within voxels (or) of tissue influenced by the intrinsic gradient. (B = external magnetic field, r = distance)

induced spin dephasing) and chemical shift dephasing (in-phase/out-of-phase effects). Motion artifacts are enhanced with increasing echo delay time (Fig. 5). Chemical shift dephasing is cyclical, depending on the echo delay selected [11], and is not observed in standard SE imaging. Chemical shift misregistration—i.e., spatial mismapping along the frequency-encoding axis—occurs in both SE and GRE imaging.

Conclusions

Magnetic susceptibility artifacts may appear in MR images when gradient-recalled echo pulse sequences are used. These artifacts distort air/tissue interfaces, bone, and ferromagnetic objects. Artifactual accentuation of spinal canal narrowing and foraminal stenosis in patients with cervical spondylosis may result in false interpretations of MR images. It is recommended that the shortest possible echo delay times be used to minimize magnetic susceptibility artifacts encountered in gradient echo MR imaging.

REFERENCES

1. *The Chemical Rubber Company handbook of chemistry and physics*, 68th ed. Boca Raton, FL: CRC, 1987–1988
2. Bellon EM, Haacke EM, Coleman PE, Sacco DC, Steiger DA, Gangarosa RE. MR artifacts: a review. *AJR* **1986**;147:1271–1281
3. Wehrli FW. Fast-scan magnetic resonance imaging: principles and contrast phenomenology. In: Higgins CB, Hricak H, eds. *Magnetic resonance imaging of the body*. New York: Raven, **1987**
4. Wehrli FW. MacFall JR, Newton TH. Parameters determining the appearance of NMR images. In: Newton TH, Potts DG, eds. *Modern neuroradiology*, vol. 2. San Anselmo, CA: Clavadel, **1983**
5. Gomori JM, Grossman RI, Goldberg HI, Zimmerman RA, Bilaniuk LT. Intracranial hematomas: imaging by high-field MR. *Radiology* **1985**;157:87–93
6. Edelman RR, Johnson K, Buxton R, et al. MR of hemorrhage: a new approach. *AJNR* **1986**;7:751–756
7. Cox IJ, Bydder GM, Gadian DG, et al. The effect of magnetic susceptibility variations in NMR imaging and NMR spectroscopy in vivo. *J Magn Reson* **1986**;70:163–168
8. *The Chemical Rubber Company handbook of chemistry and physics*, 68th ed. Boca Raton FL: CRC, 1987–1988
9. Frahm J, Haase A, Matthaei D. Rapid NMR imaging of dynamic processes using the FLASH technique. *Magn Reson Med* **1986**;3:321–327
10. Wehrli FW, Shimakawa A, Gullberg GT, MacFall JR. Time-of-flight MR flow imaging: selective saturation recovery with gradient refocusing. *Radiology* **1986**;160:781–785
11. Wehrli FW, Perkins TG, Shimakawa A, Roberts F. Chemical shift-induced amplitude modulations in images obtained with gradient refocusing. *Magn Reson Imaging* **1987**;5:157–158